NIH Public Access
Author Manuscript
Biochemistry. Author manuscript; available in PMC 2011 July 6.

Published in final edited form as:
Biochemistry. 2010 July 6; 49(26): 5511–5523. doi:10.1021/bi100157u.

Membrane localization of LRRK2 is associated with increased formation of the highly active LRRK2 dimer and changes in its phosphorylation[1]

Zdenek Berger[1,2], **Kelsey A. Smith**[1], and **Matthew J. LaVoie**[1,2]

[1] Center for Neurologic Diseases, Department of Neurology, Brigham and Women's Hospital, Boston, Massachusetts, USA

[2] Harvard Medical School, Boston, Massachusetts, USA

Abstract

Autosomal dominant mutations in the leucine rich repeat kinase 2 (LRRK2) are the most common genetic cause of Parkinson's disease (PD). Despite the presence of multiple domains, the kinase activity of LRRK2 is thought to represent the primary function of the protein. Alterations in LRRK2 kinase activity are thought to underlie the pathogenesis of its PD-linked mutations; however, many questions regarding basic aspects of LRRK2 function remain unclear, including the cellular mechanisms of LRRK2 regulation and the importance of its unique distribution within the cell. Here, we demonstrate for the first time that the subcellular localization of wild-type LRRK2 is associated with changes in four distinct biochemical properties likely crucial for LRRK2 function. Our data demonstrate for the first time that the wild-type LRRK2 dimer possesses greater kinase activity than its more abundant monomeric counterpart. Importantly, we show that this activated form of LRRK2 is substantially enriched at the membrane of cells expressing endogenous or exogenous LRRK2, and that the membrane-associated fraction of LRRK2 likewise possesses greater kinase activity than cytosolic LRRK2. In addition, membrane-associated LRRK2 binds GTP more efficiently than cytosolic LRRK2, but demonstrates a lower degree of phosphorylation. Our observations suggest that multiple events, including altered protein-protein interactions and post-translational modification, contribute to the regulation of LRRK2 function, through modulating membrane association and complex assembly. These findings may have implications for the sites of LRRK2 function within the cell, the identification and localization of bona fide LRRK2 substrates, and efforts to design small molecule inhibitors of LRRK2.

Parkinson's disease (PD) is the second most common neurodegenerative disorder, affecting ~2% of population over the age of 50, with ~1.5 million patients in the US alone (1). Mutations in multiple genes are now known to cause familial PD (2,3), paving the way for molecular approaches to study the disease. The most common mutations in PD are found in the leucine rich repeat kinase 2 (LRRK2). They account for between 5% and 40% of familial parkinsonism and for 0.5–2.0% of sporadic PD cases (2,4–6). The vast majority of cases with LRRK2 mutations present pathologically with α-synuclein inclusions, as in classic idiopathic PD (4,6), establishing the likelihood that studying LRRK2 may shed light

[1]This work was supported by an Edward R. and Anne G. Lefler Postdoctoral Fellowship (ZB), NIH grant AG023094 (MJL) and the Brigham and Women's Hospital Udall Center of Excellence for Parkinson's Disease Research (NS038375).

Correspondence should be addressed to MJL. (mlavoie@rics.bwh.harvard.edu), Phone: +1-617-525-5185, Fax: +1-617-525-5252.

SUPPORTING INFORMATION AVAILABLE

Additional analyses of LRRK2 molecular weights, kinase activity, and GTP-binding can be found in the Supplementary Information. This material is available free of charge via the Internet at http://pubs.acs.org.

NIH-PA Author Manuscript
NIH-PA Author Manuscript
NIH-PA Author Manuscript

NIH-PA Author Manuscript

NIH-PA Author Manuscript

NIH-PA Author Manuscript

on the pathogenic mechanisms underlying all PD cases. Although mutations in LRRK2 demonstrate an autosomal dominant inheritance pattern, their penetrance is age-dependent and incomplete (7–10). These observations suggest the existence of regulatory pathways that control LRRK2 activity, as is true for most kinases. However, little is known about how cells might regulate LRRK2 activity and what biochemical events would be responsible.

LRRK2 encodes a large protein of 2527 amino acids with PD-linked mutations spanning the entire protein, including its kinase and Roc (GTPase) domains (5,6,11). The kinase domain is homologous to other MAPKKKs and its activity is believed to be crucial for its function and may also be important for the pathogenic processes in PD (12–20). Immunohistochemical and electron microscopic analyses of LRRK2 revealed the presence of the protein in close proximity to numerous membranes structures in mammalian brain (21), and biochemical studies have validated the membrane association of LRRK2 (22). Interestingly, LRRK2 has been implicated in diverse cellular processes, most of which either involve membrane dynamics or occur at the membrane, such as maintenance of neurite morphology (23,24), vesicle endocytosis (25) autophagy (24,26) and Wnt signaling (27). However the importance of this subcellular localization on the biochemical properties of LRRK2 or its function has not been previously examined.

LRRK2 has been recently suggested to form a dimer (28–30) in intact cells. Furthermore, an *in vitro* study using a recombinant ROC domain fragment of LRRK2 indicated that the R1441C mutation destabilizes the LRRK2 dimer (31), implying a potential role for altered dimerization of LRRK2 in PD pathogenesis. However, there are several outstanding questions to be addressed with regards to the LRRK2 dimer, including the respective activity of monomeric and dimeric LRRK2 and whether the LRRK2 dimer possesses a specialized distribution within the cell.

Although LRRK2 is present both in the cytosol and at the membrane (21,22), it is not known whether presence of LRRK2 in different subcellular compartments is associated with meaningful consequences for LRRK2 function or activity. In the present study, we show that the LRRK2 dimer is substantially enriched at the membrane, which coincides with greater *in vitro* kinase activity of membrane-associated pool of LRRK2 compared to cytosolic LRRK2. We also demonstrate that the less abundant LRRK2 dimer is more active (per molecule) than the more abundant LRRK2 monomer. We have established further biochemical distinctions between membrane-bound and cytosolic LRRK2. Membrane-associated LRRK2 studied from multiple systems was found to bind GTP more efficiently and was also found to be phosphorylated to a lesser extent than cytosolic LRRK2. Our data suggest that subcellular localization of LRRK2 is important for its activity, complex formation, and function, and that the membrane-associated LRRK2 dimer may represent the physiologically active form of the protein.

MATERIAL AND METHODS

Cell culture

GFP-LRRK2 and myc-LRRK2 constructs containing the entire ORF of LRRK2 (generous gifts of M. Cookson) were transiently transfected into HEK293FT cells (Invitrogen) using Lipofectamine 2000 (Invitrogen) according to manufacturer's instructions. Cells were harvested in ice-cold PBS approximately 24 hours after transfection. HEK293FT cells were cultured in Dulbecco's Modified Eagle's Media (DMEM), 10% fetal bovine serum, 100 units/ml penicillin, 0.1 mg/ml Streptomycin, 0.5 mg/ml Geneticin, 2 mM L-Glutamine, 0.1 mM MEM Non-Essential Amino Acids, 1 mM MEM Sodium Pyruvate. Lymphoblasts (Coriell ID: ND06358) were cultured in RPMI 1640, 2 mM L-glutamine, 100 units/ml

NIH-PA Author Manuscript

NIH-PA Author Manuscript

NIH-PA Author Manuscript

penicillin, 0.1 mg/ml Streptomycin, 15% fetal bovine serum. The rodent midbrain dopaminergic MES23.5 (MES) cells were cultured as previously described (32).

Generation of cytosol and membrane fractions

Cells were mechanically disrupted in lysis buffer (50 mM HEPES, 150 mM NaCl, PMSF, protease inhibitors and phosphatase inhibitors I & II (Sigma), by using 20 gentle strokes of a Potter-Elvehjem homogenizer. The resulting homogenate was then drawn with an 18.5 G needle and expelled through a 27.5 G needle five times. Homogenates were subsequently centrifuged at 1,000 × g for 10 min, the pellet was discarded and the supernatant was further centrifuged at 100,000 × g for 1 hour. The 100,000 x g supernatant was used as cytosol, while the 100,000 × g pellet represented membrane fraction. For Western blot analysis, this 100,000 × g pellet was resuspended in 2× Laemmli buffer and sonicated. For all other analyses (e.g. *in vitro* kinase assay, chemical crosslinking) the 100,000 × g pellet was first extracted for 30 min on ice using the same lysis buffer supplemented with Triton-X100 (Sigma) to a final concentration 1%, unless mentioned otherwise, and then centrifuged at 10,000 × g for 10 min. The Triton-soluble supernatant constituted the membrane fraction. Following fractionation, and prior to separation by glycerol velocity gradient (see below), Triton-X100 was supplemented to the cytosol samples to the same final concentration as the membrane fractions.

Glycerol velocity gradients

Whole-cell extracts for glycerol velocity gradients were prepared by lysing cells on ice for 30 min in 0.5% Triton-X100, 50 mM HEPES pH 7.4, 150 mM NaCl, PMSF, protease inhibitors (Sigma), phosphatase inhibitors I & II (Sigma), 2 mM DTT. The lysates were subsequently centrifuged at 10,000 × g for 10 min and supernatant was used for further analysis. Comparison between centrifugation of the sample at 10,000 × g for 10 min and 100,000 × g for 1 hour revealed no differences in LRRK2 distribution across the gradient (not shown). Cytosol and membrane fractions were prepared as described above; a final concentration of 0.5% Triton-X100 was used in both cytosol and membrane fractions. Addition of 0.5% Triton-X100 to cytosol revealed no differences in LRRK2 distribution across the gradient (not shown). Glycerol gradients were prepared in 25 mM HEPES pH 7.4, 0.5% Triton-X100, 1 mM DTT. Samples were layered on top of the glycerol gradient and centrifuged at 100,000 × g for 16 hours at 4°C. Equal volumes of each glycerol fraction were analyzed by Western blot. For quantifications of relative amount of LMW/HMW LRRK2, the boundary between these fractions was defined as the fraction with the lowest intensity and fractions with lower molecular weight (typically 15%–21% glycerol) were considered as LMW and fractions corresponding to higher molecular weight (typically 25–35% glycerol) were considered as HMW LRRK2. Glycerol gradients were calibrated using commercially available standards of known molecular weight: BSA (67 kDa), LDH (140 kDa), catalase (232 kDa), ferritin (440 kDa) (GE Healthcare) and urease (Sigma) which occurs natively as a trimer and hexamer with molecular weight of 272 kDa and 545 kDa, respectively. The distribution of LRRK2 across the glycerol gradients was verified in at least three independent experiments for each condition. In order to determine which glycerol fractions contained γ secretase complex and mitochondrial complex I subunit, cells were lysed in 1% CHAPS (to retain the native assembly state for both protein complexes) and subsequently analyzed using glycerol gradients containing 1% CHAPS.

Heterologous co-immunoprecipitation (co-IP)

The expression levels of myc-LRRK2 were matched to the expression levels of GFP-LRRK2 in an independent experiment by titrating the amount of myc-LRRK2 cDNA used during transfection (for each set of plasmid DNA). The amount of DNA per transfection was kept constant by using an empty vector (pcDNA 3.1). Cell lysates were protein normalized

NIH-PA Author Manuscript

NIH-PA Author Manuscript

NIH-PA Author Manuscript

and analyzed by Western blot using anti-LRRK2 antibody (see below). Cytosol and membrane fractions in 0.1% Triton-X100 were immunoprecipitated (IPed) using agarose-conjugated anti-c-myc resin (Vector laboratories), followed by 5 washes using lysis buffer supplemented with 0.1% Triton-X100. The resin was heated to 65°C in 2× Laemmli buffer with β-mercaptoethanol for 5–10 min and samples were analyzed by Western blot. In each experiment, cells transfected with GFP-LRRK2 and empty vector were used as a control for non-specific binding of GFP-LRRK2 to the myc resin. Three independent experiments were performed to quantify relative LRRK2 dimer levels.

In vitro kinase assays

LRRK2 was IPed using anti-c-myc agarose affinity resin (Sigma, cat. no: A7470), followed by two washes in lysis buffer with 500 mM NaCl, three washes with lysis buffer (150 mM NaCl), one with lysis buffer with no detergent and one with kinase buffer (see below) without ATP. Kinase reactions were performed in 25 mM Tris pH 7.5, 5 mM β-glycerolphosphate, 0.1 mM sodium vanadate, 10 mM magnesium chloride, 50 μM cold ATP and 10 μCi γ-ATP (^{32}P) for 30 min at 30°C. The reaction was stopped by adding 4× Laemmli buffer with β-mercapthoethanol. A small aliquot was analyzed by Western blot using the Odyssey infrared imaging system (LI-COR Biosciences). The remainder of the reaction was loaded onto 6% Tris-glycine gels (Invitrogen), dried and exposed onto autoradiography film (Kodak). LRRK2 kinase activity was quantified by measuring the intensity of ^{32}P-LRRK2 on the autoradiograph and normalizing it to the amount of LRRK2 protein by Western blot. Three independent experiments were performed to determine the relative activities of cytosolic and membrane-associated LRRK2. Detailed experiments revealed that the occasional doublet pattern of LRRK2 on SDS-PAGE indeed represents two bands both corresponding to full length LRRK2. Therefore, both bands were considered for quantitative analysis, if present. The presence of the doublet did not correlate with any specific condition and was observed in both membrane and cytosol fractions.

For *in vitro* kinase assays from the glycerol gradients, the distribution of LRRK2 across each glycerol gradient was first verified by Western blot and LMW (15–19%) and HMW (25–35%) fractions from multiple gradients were then pooled and used for myc IP. Six independent experiments were conducted to assess the relative activities of LMW and HMW LRRK2. In order to ensure optimal IP conditions, each fraction was then diluted to a final concentration of 10% glycerol and concentrated using Amicon Ultra centrifuge devices with a 100 kDa cut-off. We did not observe any loss of LRRK2 following concentration, indicating no appreciable binding of LRRK2 to the filter. Of note, we observed similar results (increased kinase activity from HMW vs. LMW LRRK2) without concentrating the samples, ruling out artifacts from the concentration procedure itself.

Chemical crosslinking

Live cells were crosslinked with DSS, DST, SATP, BMOE or BMH (Pierce) at room temperature for 30 min in PBS with 10 mM EDTA, according to the manufacturer's instructions. Control samples were incubated with the vehicle (DMSO) at the same time. Cytosol and membrane fractions (final concentration 1% Triton-X100) were protein normalized prior to crosslinking, with equal volumes used. Each experiment was repeated three times. For crosslinking of glycerol gradient fractions, 15% and 29% glycerol fraction was used as LMW and HMW, respectively.

Western blot

Samples were mixed with 4× Laemmli buffer with 20% β-mercapthoethanol, heated at 65°C for 5 minutes and loaded onto Novex (Invitrogen) or Criterion (Bio-Rad) Tris-Glycine pre-cast gels. The proteins were subsequently transferred onto polyvinylidene fluoride (PVDF)

NIH-PA Author Manuscript

NIH-PA Author Manuscript

NIH-PA Author Manuscript

membranes (Millipore) and probed with anti-myc antibody (polyclonal A14 or monoclonal 9E10, 1:1,000 and 1:500, respectively; Santa Cruz Biotechnology), anti-LRRK2 (custom affinity purified polyclonal LRRK2 antibody raised against C-terminus, antigen sequence: EKHIEVRKELAEKMRRTSVE), monoclonal anti-actin (1:50,000; Sigma) or monoclonal anti-transferrin receptor (1:1,000; Zymed), monoclonal anti-GAPDH (1:20,000; Chemicon), monoclonal anti-NDUFA9 (1:1,000, Mitosciences), polyclonal anti-nicastrin (1:1,000 Sigma, N1660), polyclonal presenilin 1 NTF (1:1,000, Calbiochem). Secondary antibodies (1:2,000–1:10,000) and ECL-plus were purchased from GE Healthcare. Following ECL application, blots were exposed onto HyBlot Cl autoradiography film (Metuchen). Densitometry was calculated using AlphaEase Automatic Image Capture (Alpha Innotech). Some Western blots were developed using the Odyssey infrared imaging system (LI-COR Biosciences), including those used to quantify LRRK2 levels from *in vitro* kinase reactions. The Odyssey system was used in conjunction with an infrared anti-mouse secondary antibody (1:5,000, Rockland Immunochemicals).

Phosphoprotein analyses

Cytosolic and membrane fractions were prepared and IPed using the high-affinity anti-c-myc agarose resin (Sigma, cat. no: A7470), as described above for *in vitro* kinase assays. Samples were separated by SDS-PAGE and the gels then fixed and stained with Pro-Q® Diamond Phosphoprotein gel stain (Invitrogen), according to the manufacturer's instructions. The gel was visualized using FLA-9000 (FujiFilm, excitation 532 nm, LPG filter). Subsequently, the same gel was stained for total proteins using SYPRO® Ruby (Invitrogen) and visualized either using FLA-9000 (FujiFilm, excitation 473 nm, LPG filter) or UV transilluminator (Alpha Innotech). The relative levels of LRRK2 phosphorylation were quantified by normalizing the intensity of phospho-protein signal to the levels of total LRRK2 (SYPRO® Ruby stain or Western blot). Cytosolic and membrane fractions of both untransfected cells and myc-LRRK2 transfected cells were analyzed in parallel. Three independent experiments were performed to quantify the relative phospho-LRRK2 levels in the cytosolic and membrane fractions.

GTP binding

GTP binding was performed as previously described (33–35) with minor modifications. Samples were prepared as described above and the cytosolic fraction was supplemented with Triton-X100 to a final concentration of 1%, to match the buffer conditions of the corresponding membrane fraction. The volume of all samples was kept constant within a given experiment and we ensured that the protein levels remained below saturating capacity of the GTP resin. Prior to GTP binding, the GTP-agarose resin was blocked with 100μg/ml BSA in PBS for 1 hour. Cell lysates were incubated for 1 hour at 4°C, followed by three washes in lysis buffer with 1% Triton-X100, and then specifically bound LRRK2 was eluted with 2 mM GTP for 90 minutes. Three independent experiments were performed using both cytosol and membrane fractions.

Size exclusion chromatography

Size exclusion chromatography was carried out at 4°C using an AKTA-FPLC system (GE Healthcare). Samples were injected onto a Superdex 200 10/300 GL column (GE Healthcare) equilibrated in 50 mM HEPES pH 7.4, 150 mM NaCl (unless mentioned otherwise) and eluted using the same buffer at a flow rate of 0.2 ml/min. Fractions (0.25 ml) were analyzed by Western blot, as described above. The column was calibrated using the following standards and corresponding elution volumes: thyroglobulin (669 kDa, 9.5 ml, Bio-Rad), apoferritin (440 kDa, 11.32 ml, Sigma), catalase (232 kDa, 12.97 ml, Sigma), aldolase (158kDa, 13.37 ml, GE Healthcare), conalbumin (75 kDa, 14.67 ml, GE

NIH-PA Author Manuscript

NIH-PA Author Manuscript

NIH-PA Author Manuscript

Healthcare), ovalbumin (44 kDa, 15.63 ml, Bio-Rad), myoglobin (17 kDa, 17.59 ml, Bio-Rad). Blue dextran was used to confirm the void volume (8.79 ml, GE Healthcare).

Blue-Native PAGE

Blue-Native PAGE was performed according to manufacturer's instructions (Invitrogen) using 3–12% Bis-Tris native gels. After electrophoresis, the gel was incubated in transfer buffer containing 0.1% SDS for 10–15 minutes and subsequently transferred to PVDF in the presence of 0.01% SDS to improve the transfer efficiency of high molecular weight protein complexes. Two independent molecular weight standards were purchased from GE Healthcare and Invitrogen, respectively. In order to determine the relative migration of LRRK2, these standards were run on adjacent lanes along with LRRK2 samples and analyzed both on the gel itself (coomassie staining) and on the membrane (after transfer on the PVDF membrane and staining with Ponceau S).

Statistical analyses

Data were analyzed either by a two-tailed Student's t-test (Figures 2, 3) or by an unpaired two-tailed t-test with unequal variance (Figures 1, 4, 7). The latter was used when data were normalized to control (36).

Mice

All animals were housed and cared for under the guidelines established by Harvard University's Institutional Animal Care and Use Committees in compliance with Federal standard and fed standard chow. Cytosolic and membrane fractions were prepared from brains of C57BL/6 mice at 16 months of age, as described above.

RESULTS

Two pools of LRRK2 with distinct molecular weights are observed from whole-cell extracts

To biochemically separate independent forms of LRRK2 we employed glycerol velocity gradients (37), which separate native proteins based on relative buoyancy (molecular weight and hydrodynamic radius). Analysis of total extracts from HEK293FT cells transfected with human wild-type full-length LRRK2 (myc-tagged) revealed a biphasic distribution of LRRK2 across the gradient (Figure 1a). We termed these two distinct pools low molecular weight (LMW) and high molecular weight (HMW) LRRK2. LMW LRRK2 migrates at ~230 kDa, likely representing a monomer, while HMW LRRK2 is found at approximately double the molecular weight (~440 kDa), consistent with a LRRK2 dimer (Figure 1a). The apparent migration of the LRRK2 monomer and dimer slightly below their predicted molecular weights is likely due to the dependence of sedimentation velocity on the hydrodynamic radius of the protein.

Endogenous LRRK2 from human lymphoblasts displayed a nearly identical distribution, with two distinct pools of LRRK2 (Figure 1b). Since LRRK2 in the lymphoblasts is expressed at several-fold lower levels than that following transient transfection (Fig S1a), these data suggest that the distribution of LRRK2 across the glycerol gradient is not influenced by protein expression levels. The occasional shift in LMW or HMW LRRK2 by one fraction is likely due to the subtle variability of manual fraction collection. Similar LRRK2 distribution was observed in whole-cell lysates from the dopaminergic MES cell line transfected with LRRK2 (Figure S1b) as well as when using multiple nonionic detergents (0.1–0.5% Triton-X100, 0.5% DDM, data not shown). The addition of the denaturing detergent, SDS, to cell lysates prior to separation resulted in a complete collapse of HMW LRRK2 (Figure 1a, b; lower panels), consistent with HMW LRRK2 representing a dissociable, multimeric protein complex. The relative abundance of the LMW and HMW

NIH-PA Author Manuscript

NIH-PA Author Manuscript

NIH-PA Author Manuscript

pools of LRRK2 observed by glycerol gradient separation is also consistent with the low levels of oligomeric LRRK2 determined using heterologous co-immunoprecipitation from whole-cell lysates (Figure S1c).

In order to confirm the calibration of the glycerol gradients that was accomplished using commercial protein standards, we analyzed the sedimentation of two well-characterized, endogenous protein complexes in the same glycerol gradients. Endogenous γ-secretase complex is a protease of 230–250 kDa as determined by Blue-Native PAGE, glycerol gradients and scanning eletron transmission microscopy (38–40) and is readily identified by the presence of both a mature glycosylated form of nicastrin (mNCT) and presenilin N-terminal fragment (NTF) (41,42). Fully assembled γ-secretase was found in the 15–19% glycerol fractions (Figure 1c), similar to LMW LRRK2 (Figure 1a, b) and consistent with the calibration with multiple protein standards. Endogenous mitochondrial complex I, a multi-protein complex of 980 kDa (43) was detected in 35% glycerol (Figure 1c), consistent with our prior calibration with the protein standards. To further confirm that LMW and HMW LRRK2 represented LRRK2 monomer and dimer, respectively, HEK293FT cells were transiently co-transfected with myc-LRRK2 and GFP-LRRK2 and cell lysates were separated by glycerol gradient. LMW and HMW fractions were then IPed using a high-affinity myc-resin and probed using myc and GFP antibodies. Substantially more GFP-LRRK2 was co-IPed from the HMW than from the LMW fractions (Figure S1d), confirming that HMW LRRK2 represents the LRRK2 dimer. Consistent with this observation, LRRK2 collected from the HMW glycerol gradient fractions is efficiently crosslinked into covalent HMW SDS-stable complexes while LMW LRRK2 is not (Figure S2a).

Endogenous and transfected LRRK2 has been repeatedly observed by us (e.g. Figure 1) and others (12,28,29) as two distinct bands on Western blot. Since both bands were detectable with antibodies against both extreme C-terminus (proprietary anti-LRRK2 antibody) and two different N-terminus antibodies (monoclonal and polyclonal anti-myc), they must both represent full length LRRK2 protein (data not shown). Dephosphorylation did not affect the band migration and both bands could be observed when blotting extracts from *in vitro* transcription/translation of LRRK2 using rabbit reticulocytes (data not shown), indicating that post-translational modifications are unlikely to cause this effect. In all experiments both bands representing the full length LRRK2 protein were considered/quantified, if present.

In order to confirm the presence of multiple oligomerization states of LRRK2 by an independent method, we used live-cell crosslinking, which covalently stabilizes proteins in close proximity into SDS-stable complexes which can be readily resolved by SDS-PAGE/Western blotting. The crosslinking of live human lymphoblasts (using DSS) expressing endogenous LRRK2 led to the formation of HMW LRRK2 complexes even at relatively low (25 μM) concentrations of DSS (Figure 1d), consistent with an efficient crosslinking reaction. The same crosslinker had similar effects in live MES cells transfected with LRRK2 (Figure S2b). SDS-stable complexes migrating at similar molecular weights were also obtained following live-cell crosslinking with several other reagents (BMOE, BMH, DST, SATP), which possess different functional groups (amine and sulfhydryl) and various spacer arm lengths (4.1–16.1Å, Figure S2c). These data show that both endogenous and exogenous LRRK2 form multiple HMW complexes in live cells, indicative of multiple protein-protein interactions. These likely include interactions with other LRRK2 molecules, as well as other proteins. The presence of multiple complexes observed following crosslinking compared to the biphasic distribution of LRRK2 from the glycerol velocity gradients may reflect the ability of crosslinkers to capture both more transient and weaker interactions of LRRK2 (e.g. with substrates, co-factors, chaperones), but confirm the putative dimer as the major HMW species.

NIH-PA Author Manuscript

NIH-PA Author Manuscript

NIH-PA Author Manuscript

To examine the functional consequences of these results, we utilized a well-described LRRK2 autophosphorylation assay (12,13,15,28). Using whole cell lysates from transfected cells, we observed approximately a 2-fold increase in kinase activity of the G2019S mutation compared to WT LRRK2 and a lack of kinase activity of kinase-dead construct (Figure S2d), consistent with previous reports (12,13,15,28) and validating the assay in our hands. In order to analyze the functional consequences of LRRK2 dimer assembly, the same assay was used to compare the specific activity of LMW and HMW LRRK2 extracted from whole cell extracts, following their separation via glycerol velocity gradients. We observed an 8.4-fold increase in relative LRRK2 activity in the HMW fraction (Figure 1e), consistent with a recent publication reporting increased activity of the G2019S mutant LRRK2 dimer compared to mutant monomer (44).

High Molecular Weight LRRK2 is enriched at the membrane

Previous reports have demonstrated the presence of LRRK2 in both cytosol and membrane fractions (21,22), although the relative distribution has not been well characterized. Therefore, we fractionated cells and tissue into cytosol and membrane pools, volume-adjusted both fractions and determined the relative abundance of soluble or membrane-associated LRRK2. Analysis of HEK293FT cells transfected with LRRK2 showed that the majority of cellular LRRK2 was present in the cytosol (~75%) with a smaller amount (~25%) at the membrane. A similar distribution was observed with endogenous LRRK2 from human lymphoblasts, primate and mouse brain (Figure 2a). These data indicate that in our experimental systems, the majority of LRRK2 is present in cytosol with a smaller proportion localized to the membrane.

Next, we examined if LMW or HMW LRRK2 is preferentially enriched in either subcellular fraction. Analysis of HEK293FT cells transfected with LRRK2 revealed the presence of LMW LRRK2 in both fractions while HMW LRRK2 was almost exclusively present at the membrane (Figure 2b). Quantification of multiple experiments showed a 20-fold enrichment of HMW LRRK2 at the membrane (Figure 2b). Similar results were observed with endogenous LRRK2, with a 15-fold enrichment (Figure 2c). In order to determine if PD-linked mutations exhibited differences from the wild-type protein, we analyzed both the relative distribution in cytosolic and membrane fractions (Figure 3a, Figure S3a) and LMW/HMW distribution across the glycerol gradients (Figure 3b). Interestingly, no significant differences were observed either in cytosol or membrane fractions analyzing the R1441C, Y1699C, and G2019S PD-linked mutations, which occur in three distinct domains of LRRK2 (Figure 3).

In order to verify the enrichment of HMW LRRK2 at the membrane using an independent method, we employed co-immunoprecipitation (co-IP) of heterologously tagged LRRK2 constructs. Expression levels of myc-LRRK2 and GFP-LRRK2 were matched in prior experiments (Figure 4a), maximizing the probability of forming GFP-/myc-LRRK2 heterodimers (Fig 4b). Both GFP-LRRK2 and myc-LRRK2 were present at higher levels in the cytosol than at the membrane (Figure 4c, lanes 1 and 3), illustrating that LRRK2 localization is tag-independent and again that the majority of total LRRK2 is found in the cytosol. The previously observed ratio of soluble/membrane-associated LRRK2 was preserved in the myc immunoprecipitations (IPs) (Figure 4c, lanes 5–7), suggesting that the high affinity anti-myc resin exhibited similar capture efficiency from both fractions.

If equal amounts of LRRK2 dimer were present in cytosol and membrane fractions, one would expect the levels of co-IPed GFP-LRRK2 to mirror the pattern of myc-LRRK2: higher levels of GFP-LRRK2 from cytosol and lower levels from membranes. However, the opposite was observed. The myc resin pulled down greater levels of GFP-LRRK2 from membrane than from cytosol (Figure 4c, lane 7 vs lane 5 and 6), consistent with a greater

NIH-PA Author Manuscript

NIH-PA Author Manuscript

NIH-PA Author Manuscript

abundance of the LRRK2 dimer in the membrane fraction. This was observed despite lower levels of IPed myc-LRRK2 in this fraction (Figure 4c, lane 7). Since the relative amounts of dimer can be quantified by using the ratio of GFP-LRRK2:myc-LRRK2, an analysis across three independent experiments revealed a 5.7-fold enrichment of LRRK2 dimer in the membrane fraction compared to the cytosol (Figure 4d).

To further confirm that the HMW LRRK2 complexes were enriched at the membrane, we compared the relative efficiency of LRRK2 crosslinking in cytosol and membrane fractions using increasing concentrations of DSS. No crosslinking of endogenous LRRK2 was observed in the cytosolic fraction from lymphoblasts up to 50 μM DSS, while LRRK2 from the membrane fraction was efficiently crosslinked into HMW complexes (Figure 5a). Efficient crosslinking of LRRK2 into HMW complexes was also observed in membrane extracts from HEK293FT cells transfected with LRRK2 (Figure 5b), and from non-human primate brain extracts (Figure 5c). In contrast, LRRK2 from the cytosolic fractions consistently failed to crosslink at these concentrations (Figure 5b, c). Thus, glycerol velocity gradients, heterologous co-IP, and crosslinking all support the enrichment of the HMW LRRK2 kinase complex at the membrane with both endogenous and exogenous LRRK2 from cells and brain tissue.

There are conflicting reports on the estimated size of LRRK2 using size exclusion chromatography (SEC). While some groups have found LRRK2 to elute at ~ 600kDa (28,45), others' data suggest that most of LRRK2 elutes at a much larger size (44,46). However, one report analyzed further this very large LRRK2 pool, and concluded that it was monomer and that monomeric LRRK2 elutes aberrantly on SEC (46). Our SEC analysis of LRRK2 from cytosol, which contains almost exclusively LRRK2 monomer, suggested a molecular weight of ~ 1.3 MDa (Figure 6a), consistent with this prior report. Furthermore, a similar elution profile was observed when LMW fraction from the glycerol gradient was subsequently analyzed by SEC (Figure 6a). In our hands, HMW LRRK2 eluted at ~ 500 kDa, consistent with the approximate molecular weight of LRRK2 dimer and the prior observations that LRRK2 dimer may elute properly on SEC (46), despite the unexpected behavior of the monomer. Since we report that most of LRRK2 is present as a monomer in transfected cells, most of LRRK2 from whole-cell lysates would be expected to elute as the "abnormal" large complex, consistent with a prior report (44). We have also confirmed the apparent size of LMW and HMW LRRK2 as monomer and dimer, respectively, using Blue-Native PAGE calibrated with two different commercial molecular weight standards (Figure 6b,Figure S4a). This indicates that SEC may uniquely report an inaccurate mass of monomeric LRRK2. To address the apparent discrepancies of LRRK2 size between multiple groups (~1.3MDa vs 600 kDa) using size exclusion chromatography, we compared the elution profiles of LRRK2 from cytosol using our conditions with those previously used to estimate LRRK2 molecular weight at ~ 600 kDa (28,45). Comparison of LRRK2 elution profile in the absence or presence of Triton-X100 revealed that the addition of the detergent leads to a broader elution peak for LRRK2, thus changing its estimated molecular weight (Figure S4b), potentially accounting for some of the differences reported by various groups analyzing LRRK2 via SEC.

LRRK2 localization affects its activity and biochemical properties

To examine the functional consequences of LRRK2 localization, we utilized the well-documented LRRK2 autophosphorylation assay. We prepared cytosol and membrane fractions, IPed equal amounts of LRRK2 from both and compared their relative *in vitro* LRRK2 kinase activities. Analysis of three independent experiments revealed a 3.1-fold increase in the relative autophosphorylation activity of membrane-associated LRRK2 compared to cytosolic LRRK2 (Figure 7a). Kinase-dead LRRK2, which was present both in cytosol and membrane fractions (Figure S3b), did not exhibit significant activity from either

NIH-PA Author Manuscript

NIH-PA Author Manuscript

NIH-PA Author Manuscript

fraction (Figure S5a), confirming the specificity of the assay. Similar increases in membrane-associated kinase activity were also observed in a second assay, using myelin basic protein as a pseudosubstrate (Figure S5b). However, this assay was not exhaustively employed due to the greater variability and considerably weaker specificity for LRRK2 activity that we (not shown), and others (28), have observed.

LRRK2 can bind GTP through its COR domain (13,17,34,47,48), and GTP binding may influence the kinase activity of LRRK2 (13,49). In order to further biochemically characterize cytosolic and membrane pools of LRRK2, we compared the relative binding of LRRK2 to GTP-agarose beads using a previously established assay (13,17,34,47,48). Endogenous membrane-associated LRRK2 from lymphoblasts and primate brain exhibited greater binding to GTP resin than cytosolic LRRK2 (Figure 7b, 7c, Figure S5c, S5d). Similar results were also obtained with extracts from dopaminergic MES cells transfected with WT-LRRK2 (Figure S5e).

Kinases are often regulated by phosphorylation (50–52) and indeed multiple phosphorylation sites have been identified in LRRK2 (53,54). In the absence of phospho-specific LRRK2 antibodies, we evaluated the overall extent of LRRK2 phosphorylation in cytosolic and membrane fractions using an organic fluorophore, Pro-Q® Diamond, which binds to the phosphate moiety independent of the protein context (55). LRRK2 was IPed from both cytosolic and membrane fractions, separated on SDS-PAGE, and the LRRK2 protein was first stained with Pro-Q® Diamond Phospho-protein stain and subsequently analyzed with a total protein stain (Figure 7d). The levels of the phospho-LRRK2 were normalized to total LRRK2 to obtain the relative phosphorylation levels. Quantitative analysis of three independent experiments showed that membrane-associated LRRK2 was phosphorylated to a lesser extent (-31%) than cytosolic LRRK2 (Figure 7d).

DISCUSSION

Previous studies have established that LRRK2 is a bona fide kinase (12,13,15,28) and more recent evidence suggests that it exists as a dimer (28–30). Here we report that the less abundant LRRK2 dimer is more active than the more abundant monomer. Since LRRK2 is thought localize to membranous structures in mammalian brain (21), we hypothesized that control over subcellular localization may represent a mechanism for regulating LRRK2 function. Here, we report that the membrane association of LRRK2 is accompanied by a number of different, but likely related biochemical events. These include increased dimerization, increased kinase activity, increased GTP-binding and decreased phosphorylation (compared to cytosolic LRRK2). In summary, our data suggest that membrane targeting and dimerization of wild-type LRRK2 are critical biochemical mechanisms governing LRRK2 kinase activity, and therefore its function within the cell.

The difference in activity between cytosolic and membrane-associated wild-type LRRK2 (~3-fold) is comparable to that between the wild-type and the pathogenic G2019S mutant in whole cell lysates. This suggests that the association of LRRK2 with membranes may be as influential to LRRK2 function as at least one pathogenic mutation, and could represent a key event in the regulation of LRRK2 activity. Also, HMW LRRK2 is ~8-fold more active than LMW, suggesting that the HMW pool represents an “activated” state and that the increased kinase activity of membrane-associated LRRK2 is likely at least partly due to an enrichment of the highly active dimer.

The increased activity of membrane-associated LRRK2 was also accompanied by increased GTP-binding of endogenous LRRK2 extracted from human lymphoblasts and primate cortex. This observation may be a result of increased GTP-exchange, a tendency of

NIH-PA Author Manuscript

NIH-PA Author Manuscript

NIH-PA Author Manuscript

increased GTPase activity, or a relatively GTP-deficient state of the membrane-associated LRRK2 protein. However, these were not directly addressed in the current manuscript. Future experiments will examine these possible mechanisms, as well as the relative GTPase activities of cytosolic and membrane-associated LRRK2, and kinetics parameters of these biochemically distinct pools of LRRK2, as recently reported (56–58).

We report decreased phosphorylation of the membrane-associated LRRK2 compared to cytosolic LRRK2, which suggests that dephosphorylation at certain sites may represent a requisite step in increased LRRK2 activity, dimer formation, trafficking to the membrane, or a combination of these processes. These data are consistent with a widely accepted model in which phosphorylation of kinases regulates their function (50–52). Importantly, since LRRK2 is a large kinase with 103 predicted phosphorylation sites (77 Ser, 15 Thr, 11 Tyr, http://www.cbs.dtu.dk/services/NetPhos/) (59), the ~30% decrease in membrane LRRK2 phosphorylation may represent a major change in a small subset of these sites, that may correlate with subcellular localization. Future analysis of specific LRRK2 phosphorylation sites (53,54) using mass spectrometry or LRRK2 phospho-specific antibodies may help identify which amino acid residues are involved in these processes and dissect the precise consequences of their phosphorylation on LRRK2 function.

Several studies have analyzed the molecular weight distribution of LRRK2 by size exclusion chromatography (SEC) with varying results. While some have reported substantial levels of LRRK2 above 1 MDa, all groups have failed to observe a pool of LRRK2 at the predicted molecular weight of a monomer. Early studies thus concluded that most LRRK2 exists as a HMW complex (28,45). However, recent work has analyzed the very HMW LRRK2 species and concluded that it is in fact an anomalously-eluting monomer (46), consistent with our SEC data (Figures 6,S4) and glycerol velocity gradient analyses (Figures 1,2). In addition, our data reporting an ~8-fold greater kinase activity of the LRRK2 dimer compared to monomer (separated by glycerol gradients) is consistent with the work from another group that found ~6-fold greater kinase activity of the LRRK2 dimer compared to very HMW LRRK2 from the SEC void volume, which we (Figures 6,S4) and others have likewise defined as monomer (46). Based on the data obtained from multiple separation methods, we speculate that the LRRK2 monomer may exist as a relatively diffuse structure whereas the LRRK2 dimer may possess a more compacted/globular structure more amenable to separation via SEC. This interpretation is analogous to the aberrant migration of linear dextran standards compared to biological protein standards. While the LRRK2 monomer was identified by glycerol velocity gradients and Blue-Native PAGE, and subsequently confirmed by heterologous co-IP and crosslinking, the aberrant migration of LRRK2 monomer observed by us and others will warrant further examination.

Interestingly, the G2019S mutant shows increased kinase activity (Fig. S2d and 12,13,15,28) without detectable changes in its subcellular localization or LMW/HMW distribution (Figure 3). This is likely due to the fact that the G2019 residue sits within the kinase domain, and directly affects kinetic properties of the kinase moiety. While a previous study using full length and truncated LRRK2 species suggested that the R1441C mutation may destabilize a LRRK2 heterodimer (31), we did not observe any significant differences in HMW/dimer levels using three various full length PD-linked mutants (including R1441C), suggesting that mutations in the context of full-length LRRK2 may not lead to substantially different dimer levels at steady state. Our data contrast with a previous report (44) suggesting differences between wild-type and G2019S in the levels of their respective dimers. These differences may be attributed to differences in the extraction protocol – we used detergents to extract membrane-associated LRRK2 (the major source of LRRK2 dimer) while the previous report employed cycles of freeze/thawing in a detergent-free condition, which may not completely extract LRRK2 from the membrane, thus accounting for the differences observed. However,

NIH-PA Author Manuscript

NIH-PA Author Manuscript

NIH-PA Author Manuscript

we cannot rule out the possibility that smaller differences between wild-type LRRK2 and mutants exist or that other related features, such as the kinetics of dimerization or the intrinsic stability of PD-linked mutant dimers may differ.

Our observation of greater *in vitro* LRRK2 kinase activity from membrane preparations leads us to speculate that the membrane compartment is likely the site where LRRK2 exerts its physiologically relevant function in the cell. Indeed, many cellular processes that are influenced by LRRK2 occur at the membrane or involve membrane dynamics (23–27,60). We suggest that LRRK2 is predominantly found as a monomer in the cytosol, but can translocate to the membrane, subsequently dimerize, and thus possesses greater kinase activity (Figure 8). This LRRK2 model is similar to that of a well-studied canonical MAPKKK Raf, which can phosphorylate its target proteins at the membrane and is regulated by dimerization, membrane-association, and phosphorylation (52,61).

Interestingly, the relatively small proportion of LRRK2 dimer in whole cell extracts implies a low level of basal kinase activity. This interpretation is supported by the relatively low rate of ^{32}P incorporation in various LRRK2 kinase assays and consistent with the relatively low basal (unstimulated) activity of other MAPKKKs (52). Therefore, identification of events leading to membrane translocation and/or formation of LRRK2 dimer may provide critical insights into LRRK2 biology. The discovery of such events may help uncover differences between wild-type and pathogenic LRRK2 proteins, which we (Figure 3) and others (18,19,22) have failed to observe at resting states with non-G2019S mutants. It is reasonable to suggest that membrane translocation and dimerization are reversible and regulated events, which represent key mechanisms for the cell to regulate LRRK2 activity. Since penetrance of the autosomally dominant inherited LRRK2 mutations is incomplete and age-dependent (7–10), regulation of LRRK2 activity is likely to be highly complex and potentially relevant to the emergence of PD pathogenesis.

In summary, we propose a novel mechanism of regulating LRRK2 function through its membrane localization and dimerization. Our findings have implications for the identification of substrates, the biochemical composition and nature of active LRRK2, and LRRK2 function within the cell. Additional work will be required, however, to elucidate the pathological relevance of these findings in the context of PD-linked mutants specifically within the neuronal environment.

Supplementary Material

Refer to Web version on PubMed Central for supplementary material.

Acknowledgments

We would like to thank Dr. Mark Cookson (NIA) for providing the LRRK2 plasmids, the New England Primate Research Facility for providing the non-human primate cortex tissue, Drs Justus Dächsel and Matthew J. Farrer for technical advice, and the Coriell Institute for Biomedical Research for providing lymphoblasts.

Abbreviations

KD	kinase dead
LMW	low molecular weight
LRRK2	leucine rich repeat kinase
MBP	myelin basic protein

NIH-PA Author Manuscript

NIH-PA Author Manuscript

NIH-PA Author Manuscript

IP	immunoprecipitation
GDP	guanosine-diphosphate
GTP	guanosinetriphosphate
HMW	high molecular weight
PD	Parkinson's disease

References

1. Thomas B, Beal MF. Parkinson's disease. Human molecular genetics. 2007; 16(Spec No 2):R183–194. [PubMed: 17911161]
2. Farrer MJ. Genetics of Parkinson disease: paradigm shifts and future prospects. Nat Rev Genet. 2006; 7:306–318. [PubMed: 16543934]
3. Cookson MR, Xiromerisiou G, Singleton A. How genetics research in Parkinson's disease is enhancing understanding of the common idiopathic forms of the disease. Current opinion in neurology. 2005; 18:706–711. [PubMed: 16280683]
4. Melrose H. Update on the functional biology of Lrrk2. Future Neurol. 2008; 3:669–681. [PubMed: 19225574]
5. Paisan-Ruiz C, Jain S, Evans EW, Gilks WP, Simon J, van der Brug M, Lopez de Munain A, Aparicio S, Gil AM, Khan N, Johnson J, Martinez JR, Nicholl D, Carrera IM, Pena AS, de Silva R, Lees A, Marti-Masso JF, Perez-Tur J, Wood NW, Singleton AB. Cloning of the gene containing mutations that cause PARK8-linked Parkinson's disease. Neuron. 2004; 44:595–600. [PubMed: 15541308]
6. Zimprich A, Biskup S, Leitner P, Lichtner P, Farrer M, Lincoln S, Kachergus J, Hulihan M, Uitti RJ, Calne DB, Stoessl AJ, Pfeiffer RF, Patenge N, Carbajal IC, Vieregge P, Asmus F, Muller-Myhsok B, Dickson DW, Meitinger T, Strom TM, Wszolek ZK, Gasser T. Mutations in LRRK2 cause autosomal-dominant parkinsonism with pleomorphic pathology. Neuron. 2004; 44:601–607. [PubMed: 15541309]
7. Healy DG, Falchi M, O'Sullivan SS, Bonifati V, Durr A, Bressman S, Brice A, Aasly J, Zabetian CP, Goldwurm S, Ferreira JJ, Tolosa E, Kay DM, Klein C, Williams DR, Marras C, Lang AE, Wszolek ZK, Berciano J, Schapira AH, Lynch T, Bhatia KP, Gasser T, Lees AJ, Wood NW. Phenotype, genotype, and worldwide genetic penetrance of LRRK2-associated Parkinson's disease: a case-control study. Lancet neurology. 2008; 7:583–590. [PubMed: 18539534]
8. Hulihan MM, Ishihara-Paul L, Kachergus J, Warren L, Amouri R, Elango R, Prinjha RK, Upmanyu R, Kefi M, Zouari M, Sassi SB, Yahmed SB, El Euch-Fayeche G, Matthews PM, Middleton LT, Gibson RA, Hentati F, Farrer MJ. LRRK2 Gly2019Ser penetrance in Arab-Berber patients from Tunisia: a case-control genetic study. Lancet neurology. 2008; 7:591–594. [PubMed: 18539535]
9. Latourelle JC, Sun M, Lew MF, Suchowersky O, Klein C, Golbe LI, Mark MH, Growdon JH, Wooten GF, Watts RL, Guttman M, Racette BA, Perlmutter JS, Ahmed A, Shill HA, Singer C, Goldwurm S, Pezzoli G, Zini M, Saint-Hilaire MH, Hendricks AE, Williamson S, Nagle MW, Wilk JB, Massood T, Huskey KW, Laramie JM, DeStefano AL, Baker KB, Itin I, Litvan I, Nicholson G, Corbett A, Nance M, Drasby E, Isaacson S, Burn DJ, Chinnery PF, Pramstaller PP, Al-hinti J, Moller AT, Ostergaard K, Sherman SJ, Roxburgh R, Snow B, Slevin JT, Cambi F, Gusella JF, Myers RH. The Gly2019Ser mutation in LRRK2 is not fully penetrant in familial Parkinson's disease: the GenePD study. BMC Med. 2008; 6:32. [PubMed: 18986508]
10. Kay DM, Kramer P, Higgins D, Zabetian CP, Payami H. Escaping Parkinson's disease: a neurologically healthy octogenarian with the LRRK2 G2019S mutation. Mov Disord. 2005; 20:1077–1078. [PubMed: 16001413]
11. Greggio E, Cookson MR. Leucine-rich repeat kinase 2 mutations and Parkinson's disease: three questions. ASN Neuro. 2009; 1
12. West AB, Moore DJ, Biskup S, Bugayenko A, Smith WW, Ross CA, Dawson VL, Dawson TM. Parkinson's disease-associated mutations in leucine-rich repeat kinase 2 augment kinase activity.

NIH-PA Author Manuscript

NIH-PA Author Manuscript

NIH-PA Author Manuscript

Proceedings of the National Academy of Sciences of the United States of America. 2005; 102:16842–16847. [PubMed: 16269541]

13. Smith WW, Pei Z, Jiang H, Dawson VL, Dawson TM, Ross CA. Kinase activity of mutant LRRK2 mediates neuronal toxicity. Nature neuroscience. 2006; 9:1231–1233.
14. Iaccarino C, Crosio C, Vitale C, Sanna G, Carri MT, Barone P. Apoptotic mechanisms in mutant LRRK2-mediated cell death. Human molecular genetics. 2007; 16:1319–1326. [PubMed: 17409193]
15. Greggio E, Jain S, Kingsbury A, Bandopadhyay R, Lewis P, Kaganovich A, van der Brug MP, Beilina A, Blackinton J, Thomas KJ, Ahmad R, Miller DW, Kesavapany S, Singleton A, Lees A, Harvey RJ, Harvey K, Cookson MR. Kinase activity is required for the toxic effects of mutant LRRK2/dardarin. Neurobiology of disease. 2006; 23:329–341. [PubMed: 16750377]
16. Lin X, Parisiadou L, Gu XL, Wang L, Shim H, Sun L, Xie C, Long CX, Yang WJ, Ding J, Chen ZZ, Gallant PE, Tao-Cheng JH, Rudow G, Troncoso JC, Liu Z, Li Z, Cai H. Leucine-rich repeat kinase 2 regulates the progression of neuropathology induced by Parkinson's-disease-related mutant alpha-synuclein. Neuron. 2009; 64:807–827. [PubMed: 20064389]
17. West AB, Moore DJ, Choi C, Andrabi SA, Li X, Dikeman D, Biskup S, Zhang Z, Lim KL, Dawson VL, Dawson TM. Parkinson's disease-associated mutations in LRRK2 link enhanced GTP-binding and kinase activities to neuronal toxicity. Human molecular genetics. 2007; 16:223–232. [PubMed: 17200152]
18. Anand VS, Reichling LJ, Lipinski K, Stochaj W, Duan W, Kelleher K, Pungaliya P, Brown EL, Reinhart PH, Somberg R, Hirst WD, Riddle SM, Braithwaite SP. Investigation of leucine-rich repeat kinase 2 : enzymological properties and novel assays. FEBS J. 2009; 276:466–478. [PubMed: 19076219]
19. Luzon-Toro B, de la Torre ER, Delgado A, Perez-Tur J, Hilfiker S. Mechanistic insight into the dominant mode of the Parkinson's disease-associated G2019S LRRK2 mutation. Human molecular genetics. 2007; 16:2031–2039. [PubMed: 17584768]
20. Gloeckner CJ, Schumacher A, Boldt K, Ueffing M. The Parkinson disease-associated protein kinase LRRK2 exhibits MAPKKK activity and phosphorylates MKK3/6 and MKK4/7, in vitro. J Neurochem. 2009; 109:959–968. [PubMed: 19302196]
21. Biskup S, Moore DJ, Celsi F, Higashi S, West AB, Andrabi SA, Kurkinen K, Yu SW, Savitt JM, Waldvogel HJ, Faull RL, Emson PC, Torp R, Ottersen OP, Dawson TM, Dawson VL. Localization of LRRK2 to membranous and vesicular structures in mammalian brain. Annals of neurology. 2006; 60:557–569. [PubMed: 17120249]
22. Hatano T, Kubo S, Imai S, Maeda M, Ishikawa K, Mizuno Y, Hattori N. Leucine-rich repeat kinase 2 associates with lipid rafts. Human molecular genetics. 2007; 16:678–690. [PubMed: 17341485]
23. MacLeod D, Dowman J, Hammond R, Leete T, Inoue K, Abeliovich A. The familial Parkinsonism gene LRRK2 regulates neurite process morphology. Neuron. 2006; 52:587–593. [PubMed: 17114044]
24. Plowey ED, Cherra SJ 3rd, Liu YJ, Chu CT. Role of autophagy in G2019S-LRRK2-associated neurite shortening in differentiated SH-SY5Y cells. J Neurochem. 2008
25. Shin N, Jeong H, Kwon J, Heo HY, Kwon JJ, Yun HJ, Kim CH, Han BS, Tong Y, Shen J, Hatano T, Hattori N, Kim KS, Chang S, Seol W. LRRK2 regulates synaptic vesicle endocytosis. Experimental cell research. 2008; 314:2055–2065. [PubMed: 18445495]
26. Alegre-Abarrategui J, Christian H, Lufino M, Mutihac R, Lourenco Venda L, Ansorge O, Wade-Martins R. LRRK2 regulates autophagic activity and localises to specific membrane microdomains in a novel human genomic reporter cellular model. Human molecular genetics. 2009
27. Sancho RM, Law BM, Harvey K. Mutations in the LRRK2 Roc-COR tandem domain link Parkinson's disease to Wnt signalling pathways. Human molecular genetics. 2009
28. Greggio E, Zambrano I, Kaganovich A, Beilina A, Taymans JM, Daniels V, Lewis P, Jain S, Ding J, Syed A, Thomas KJ, Baekelandt V, Cookson MR. The Parkinson disease-associated leucine-rich repeat kinase 2 (LRRK2) is a dimer that undergoes intramolecular autophosphorylation. The Journal of biological chemistry. 2008; 283:16906–16914. [PubMed: 18397888]

NIH-PA Author Manuscript

NIH-PA Author Manuscript

NIH-PA Author Manuscript

29. Gloeckner CJ, Kinkl N, Schumacher A, Braun RJ, O'Neill E, Meitinger T, Kolch W, Prokisch H, Ueffing M. The Parkinson disease causing LRRK2 mutation I2020T is associated with increased kinase activity. Human molecular genetics. 2006; 15:223–232. [PubMed: 16321986]
30. Klein CL, Rovelli G, Springer W, Schall C, Gasser T, Kahle PJ. Homo- and heterodimerization of ROCO kinases: LRRK2 kinase inhibition by the LRRK2 ROCO fragment. J Neurochem. 2009
31. Deng J, Lewis PA, Greggio E, Sluch E, Beilina A, Cookson MR. Structure of the ROC domain from the Parkinson's disease-associated leucine-rich repeat kinase 2 reveals a dimeric GTPase. Proceedings of the National Academy of Sciences of the United States of America. 2008; 105:1499–1504. [PubMed: 18230735]
32. LaVoie MJ, Ostaszewski BL, Weihofen A, Schlossmacher MG, Selkoe DJ. Dopamine covalently modifies and functionally inactivates parkin. Nature medicine. 2005; 11:1214–1221.
33. Li X, Tan YC, Poulose S, Olanow CW, Huang XY, Yue Z. Leucine-rich repeat kinase 2 (LRRK2)/PARK8 possesses GTPase activity that is altered in familial Parkinson's disease R1441C/G mutants. J Neurochem. 2007; 103:238–247. [PubMed: 17623048]
34. Greggio E, Lewis PA, van der Brug MP, Ahmad R, Kaganovich A, Ding J, Beilina A, Baker AK, Cookson MR. Mutations in LRRK2/dardarin associated with Parkinson disease are more toxic than equivalent mutations in the homologous kinase LRRK1. J Neurochem. 2007; 102:93–102. [PubMed: 17394548]
35. Korr D, Toschi L, Donner P, Pohlenz HD, Kreft B, Weiss B. LRRK1 protein kinase activity is stimulated upon binding of GTP to its Roc domain. Cellular signalling. 2006; 18:910–920. [PubMed: 16243488]
36. Ruxton GD. The unequal variance t-test is an underused alternative to Student's t-test and the Mann-Whitney U-test. Behavioral Ecology. 2006; 17:688–690.
37. Picton C, Klee CB, Cohen P. Phosphorylase kinase from rabbit skeletal muscle: identification of the calmodulin-binding subunits. Eur J Biochem. 1980; 111:553–561. [PubMed: 6780343]
38. LaVoie MJ, Fraering PC, Ostaszewski BL, Ye W, Kimberly WT, Wolfe MS, Selkoe DJ. Assembly of the gamma-secretase complex involves early formation of an intermediate subcomplex of Aph-1 and nicastrin. The Journal of biological chemistry. 2003; 278:37213–37222. [PubMed: 12857757]
39. Osenkowski P, Li H, Ye W, Li D, Aeschbach L, Fraering PC, Wolfe MS, Selkoe DJ. Cryoelectron microscopy structure of purified gamma-secretase at 12 A resolution. J Mol Biol. 2009; 385:642–652. [PubMed: 19013469]
40. Gu Y, Sanjo N, Chen F, Hasegawa H, Petit A, Ruan X, Li W, Shier C, Kawarai T, Schmitt-Ulms G, Westaway D, St George-Hyslop P, Fraser PE. The presenilin proteins are components of multiple membrane-bound complexes that have different biological activities. The Journal of biological chemistry. 2004; 279:31329–31336. [PubMed: 15123598]
41. Kimberly WT, LaVoie MJ, Ostaszewski BL, Ye W, Wolfe MS, Selkoe DJ. Complex N-linked glycosylated nicastrin associates with active gamma-secretase and undergoes tight cellular regulation. The Journal of biological chemistry. 2002; 277:35113–35117. [PubMed: 12130643]
42. Kimberly WT, LaVoie MJ, Ostaszewski BL, Ye W, Wolfe MS, Selkoe DJ. Gamma-secretase is a membrane protein complex comprised of presenilin, nicastrin, Aph-1, and Pen-2. Proceedings of the National Academy of Sciences of the United States of America. 2003; 100:6382–6387. [PubMed: 12740439]
43. Janssen RJ, Nijtmans LG, van den Heuvel LP, Smeitink JA. Mitochondrial complex I: structure, function and pathology. J Inherit Metab Dis. 2006; 29:499–515. [PubMed: 16838076]
44. Sen S, Webber PJ, West AB. Dependence of leucine-rich repeat kinase 2 (LRRK2) kinase activity on dimerization. The Journal of biological chemistry. 2009; 284:36346–36356. [PubMed: 19826009]
45. Klein CL, Rovelli G, Springer W, Schall C, Gasser T, Kahle PJ. Homo- and heterodimerization of ROCO kinases: LRRK2 kinase inhibition by the LRRK2 ROCO fragment. J Neurochem. 2009; 111:703–715. [PubMed: 19712061]
46. Jorgensen ND, Peng Y, Ho CC, Rideout HJ, Petrey D, Liu P, Dauer WT. The WD40 domain is required for LRRK2 neurotoxicity. PLoS One. 2009; 4:e8463. [PubMed: 20041156]

NIH-PA Author Manuscript

NIH-PA Author Manuscript

NIH-PA Author Manuscript

47. Lewis PA, Greggio E, Beilina A, Jain S, Baker A, Cookson MR. The R1441C mutation of LRRK2 disrupts GTP hydrolysis. Biochemical and biophysical research communications. 2007; 357:668–671. [PubMed: 17442267]
48. Ito G, Okai T, Fujino G, Takeda K, Ichijo H, Katada T, Iwatsubo T. GTP binding is essential to the protein kinase activity of LRRK2, a causative gene product for familial Parkinson's disease. Biochemistry. 2007; 46:1380–1388. [PubMed: 17260967]
49. Guo L, Gandhi PN, Wang W, Petersen RB, Wilson-Delfosse AL, Chen SG. The Parkinson's disease-associated protein, leucine-rich repeat kinase 2 (LRRK2), is an authentic GTPase that stimulates kinase activity. Experimental cell research. 2007; 313:3658–3670. [PubMed: 17706965]
50. Gallo KA, Johnson GL. Mixed-lineage kinase control of JNK and p38 MAPK pathways. Nat Rev Mol Cell Biol. 2002; 3:663–672. [PubMed: 12209126]
51. Ramos JW. The regulation of extracellular signal-regulated kinase (ERK) in mammalian cells. The international journal of biochemistry & cell biology. 2008; 40:2707–2719.
52. Kyriakis JM, Avruch J. Mammalian mitogen-activated protein kinase signal transduction pathways activated by stress and inflammation. Physiol Rev. 2001; 81:807–869. [PubMed: 11274345]
53. Greggio E, Taymans JM, Zhen EY, Ryder J, Vancraenenbroeck R, Beilina A, Sun P, Deng J, Jaffe H, Baekelandt V, Merchant K, Cookson MR. The Parkinson's disease kinase LRRK2 autophosphorylates its GTPase domain at multiple sites. Biochemical and biophysical research communications. 2009; 389:449–454. [PubMed: 19733152]
54. Kamikawaji S, Ito G, Iwatsubo T. Identification of the autophosphorylation sites of LRRK2. Biochemistry. 2009; 48:10963–10975. [PubMed: 19824698]
55. Goodman T, Schulenberg B, Steinberg TH, Patton WF. Detection of phosphoproteins on electroblot membranes using a small-molecule organic fluorophore. Electrophoresis. 2004; 25:2533–2538. [PubMed: 15300773]
56. Liu M, Dobson B, Glicksman MA, Yue Z, Stein RL. Kinetic mechanistic studies of wild-type leucine-rich repeat kinase 2: characterization of the kinase and GTPase activities. Biochemistry. 49:2008–2017. [PubMed: 20146535]
57. Lovitt B, Vanderporten EC, Sheng Z, Zhu H, Drummond J, Liu Y. Differential effects of divalent manganese and magnesium on the kinase activity of leucine-rich repeat kinase 2 (LRRK2). Biochemistry. 49:3092–3100. [PubMed: 20205471]
58. Nichols RJ, Dzamko N, Hutti JE, Cantley LC, Deak M, Moran J, Bamborough P, Reith AD, Alessi DR. Substrate specificity and inhibitors of LRRK2, a protein kinase mutated in Parkinson's disease. The Biochemical journal. 2009; 424:47–60. [PubMed: 19740074]
59. Blom N, Gammeltoft S, Brunak S. Sequence and structure-based prediction of eukaryotic protein phosphorylation sites. Journal of molecular biology. 1999; 294:1351–1362. [PubMed: 10600390]
60. Liou AK, Leak RK, Li L, Zigmond MJ. Wild-type LRRK2 but not its mutant attenuates stress-induced cell death via ERK pathway. Neurobiology of disease. 2008; 32:116–124. [PubMed: 18675914]
61. Raman M, Chen W, Cobb MH. Differential regulation and properties of MAPKs. Oncogene. 2007; 26:3100–3112. [PubMed: 17496909]

NIH-PA Author Manuscript

NIH-PA Author Manuscript

NIH-PA Author Manuscript

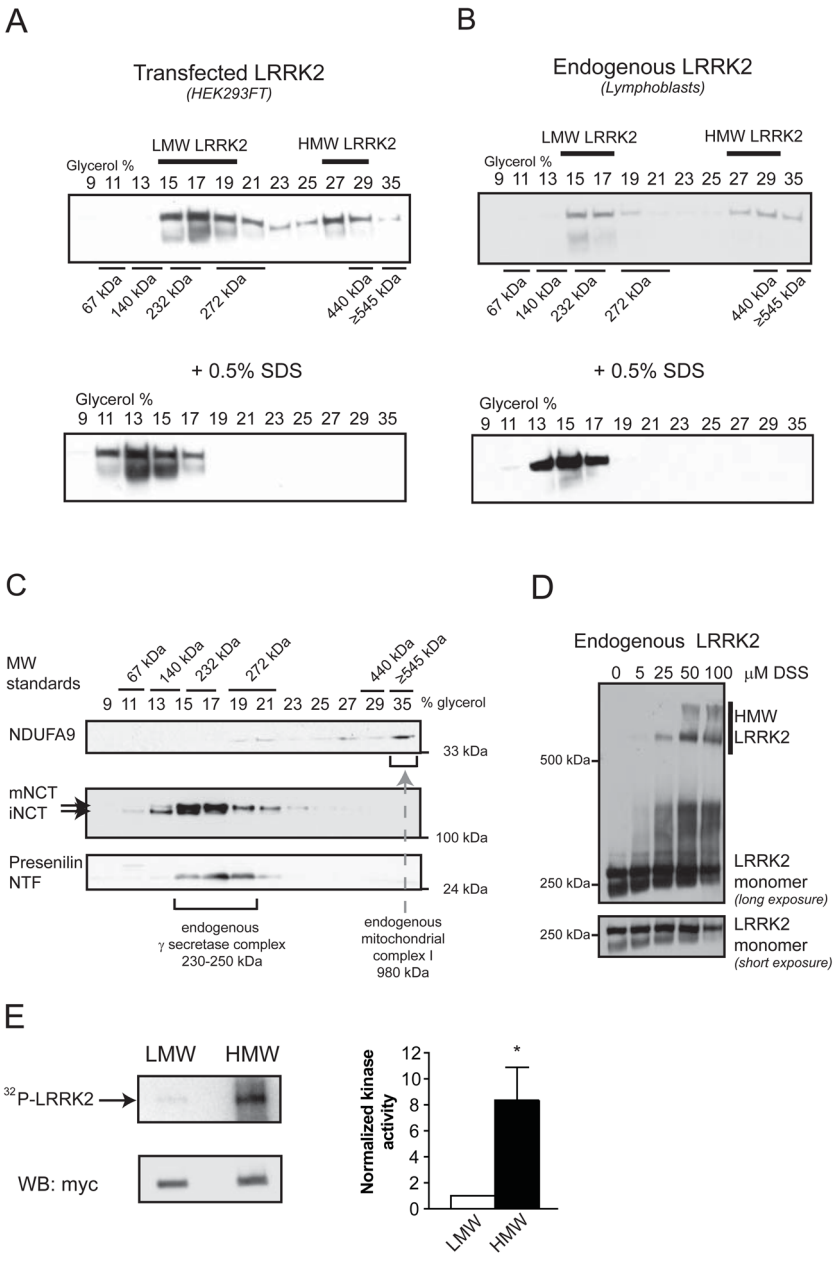

Figure 1. Analysis of HMW and LMW pools of LRRK2 and their associated kinase activity from whole-cell lysates

(**A**) Transiently transfected myc-LRRK2 from whole cell lysates is present in two distinct pools, as assessed by glycerol velocity gradients - low molecular weight (LMW) and high molecular weight (HMW). Glycerol gradients were calibrated using commercially available proteins of known molecular weight. Western blots from glycerol gradient fractions show that LMW LRRK2 migrates at ~230 kDa, likely representing a monomer, while HMW LRRK2 is found at approximately double the molecular weight (~440 kDa), consistent with a dimer. Addition of 0.5% SDS prior to glycerol gradients collapses HMW LRRK2.

(**B**) Endogenous LRRK2 from human lymphoblasts is present in two distinct pools (LMW, HMW), similar to transfected LRRK2. Western blots from glycerol gradient fractions were probed with anti-myc (A) and anti-LRRK2 antibodies (B).

NIH-PA Author Manuscript

NIH-PA Author Manuscript

NIH-PA Author Manuscript

(**C**) Endogenous γ-secretase complex, a protease of 230–250 kDa, is present in the same glycerol gradient fractions (15–19%) as LMW LRRK2. Cell lysates of HEK293FT cells transfected with myc-LRRK2 were separated using glycerol velocity gradients and analyzed using Western blots for endogenous components of the γ-secretase complex. Immature nicastrin (iNCT) undergoes further glycosylation to generate mature nicastrin (mNCT); only mNCT is part of the fully assembled γ-secretase complex. The N-terminal fragment of presenilin (NTF) is also selectively present in the fully assembled γ-secretase complex. Mitochondrial complex I (980kDa) is found in 35% glycerol, as evidenced by the presence of one its subunits - endogenous NDUFA9.
(**D**) Chemical crosslinking of live cells leads to the formation of HMW complexes of endogenous LRRK2. Live lymphoblasts expressing endogenous LRRK2 were crosslinked with increasing concentrations of DSS, leading to a dose-dependent formation of SDS-stable HMW LRRK2 complexes.
(**E**) HMW LRRK2 is more active than LMW. Wild-type myc-LRRK2 from transfected HEK293FT cells was separated into LMW and HMW pools using glycerol gradients, IPed using myc resin and subjected to an autophosphorylation assay of kinase activity. An autoradiograph of an SDS-PAGE gel separating the LRRK2 kinase reaction products shows increased incorporation of radioactive ^{32}P into HMW LRRK2 compared to LMW LRRK2. Similar levels of LRRK2 were present in both reactions, as analyzed by Western blot. Relative kinase activity of HMW LRRK2 is 8.4-fold greater than that of LMW LRRK2 (Mean ± SEM, $p = 0.03$, n = 6, unpaired t-test). * $p < 0.05$.

NIH-PA Author Manuscript
NIH-PA Author Manuscript
NIH-PA Author Manuscript

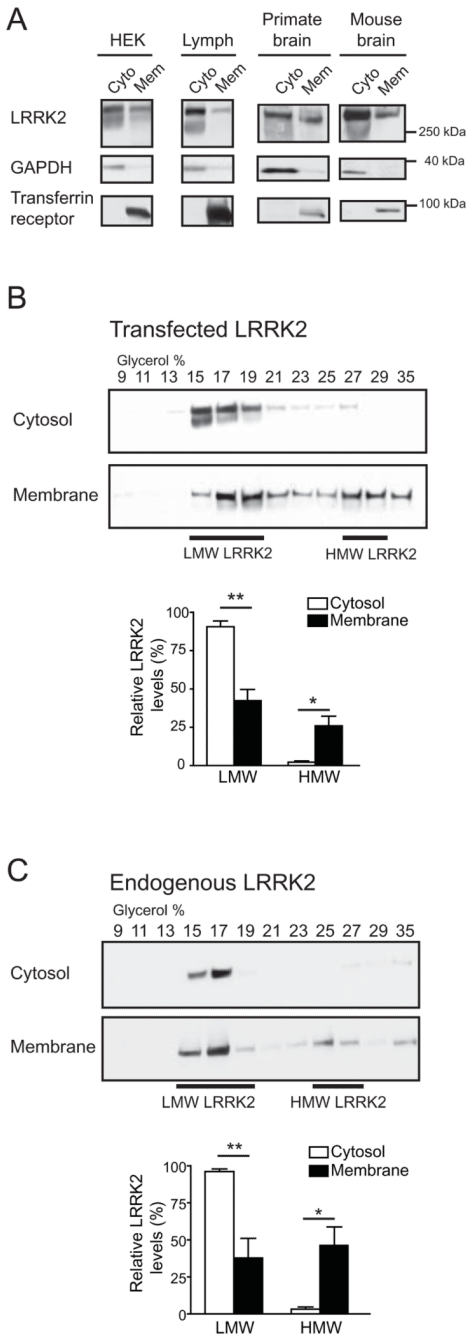

Figure 2. The high molecular weight LRRK2 complex is enriched at the membrane

(**A**) A higher proportion of LRRK2 is localized in cytosol than at the membrane. HEK293FT cells (HEK), lymphoblasts (Lymph), primate or mouse brains were homogenized and fractionated into cytosol (Cyto) and membrane (Mem) fractions. Both fractions were volume-normalized and analyzed by SDS-PAGE/Western blot. GAPDH and transferrin receptor were used as controls for proteins in the cytosol and membrane fractions, respectively.

(**B**) Glycerol gradients of cytosol and membrane extracts from HEK293FT cells transfected with myc-LRRK2 reveal a 20-fold enrichment of HMW LRRK2 at the membrane compared to the cytosol ($p = 0.02$). A higher proportion of LMW LRRK2 is found in the cytosol than

in the membrane compartment (Mean ± SEM, $p = 0.004$, n = 4, Student's t-test). * $p < 0.05$, ** $p \leq 0.01$.

(**C**) Analysis of endogenous LRRK2 from human lymphoblasts reveals an enrichment of its HMW complex at the membrane, similar to that observed in (B) with transfected LRRK2. The levels of HMW LRRK2 are 15-fold higher in membrane than cytosolic fractions (Mean ± SEM, $p = 0.01$, n = 4, Student's t-test). * $p < 0.05$, ** $p \leq 0.01$.

NIH-PA Author Manuscript
NIH-PA Author Manuscript
NIH-PA Author Manuscript

NIH-PA Author Manuscript

NIH-PA Author Manuscript

NIH-PA Author Manuscript

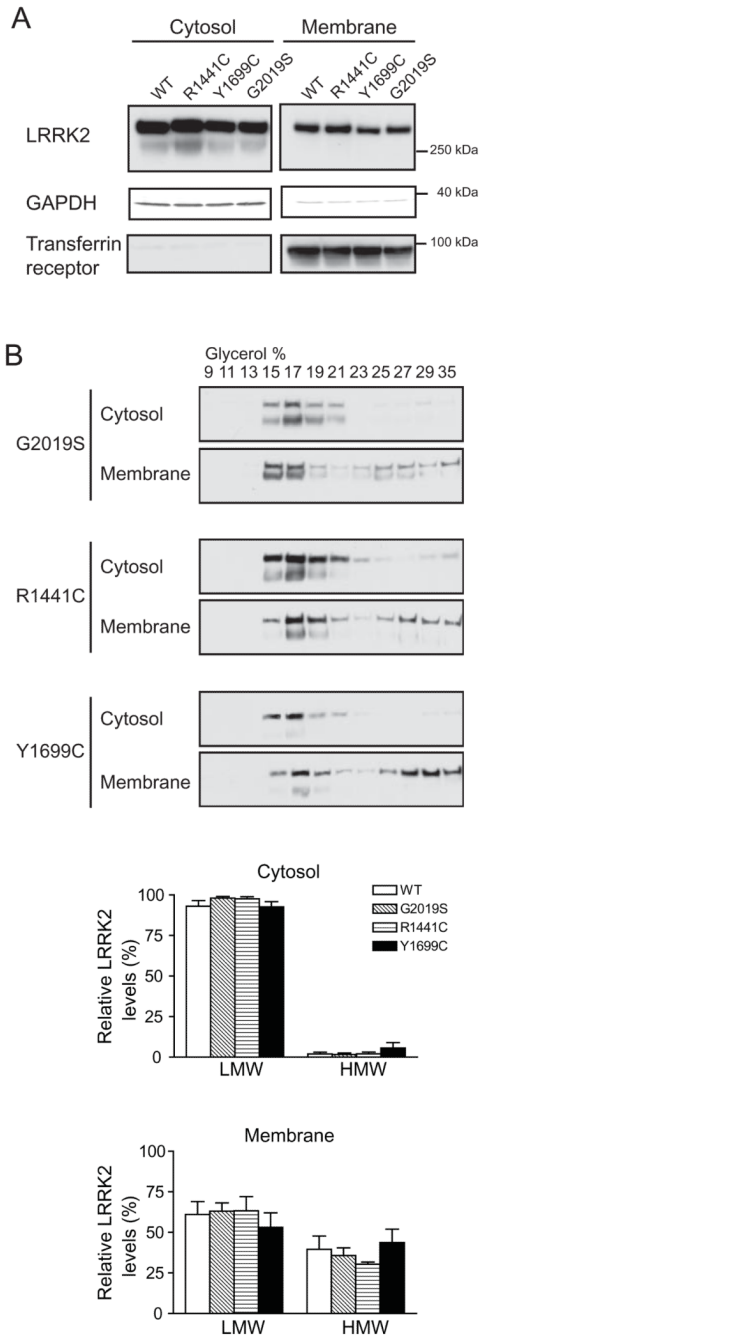

Figure 3. PD-linked mutants do not influence the subcellular localization or oligomerization state of LRRK2

(**A**) PD-linked LRRK2 mutants and wild-type LRRK2 show similar distribution across the cytosol and membrane compartments when expressed in HEK293FT cells.

(**B**) Glycerol gradients of cytosol and membrane fractions from HEK293FT cells transfected with PD-linked LRRK2 mutants. The distribution of LMW and HMW LRRK2 in either cytosol or membrane fractions is not significantly changed by the introduction of PD-linked LRRK2 mutations (G2019S, R1441C, Y1699C) (Mean ± SEM, n = 3, Student's t-test, all $p > 0.05$).

NIH-PA Author Manuscript

NIH-PA Author Manuscript

NIH-PA Author Manuscript

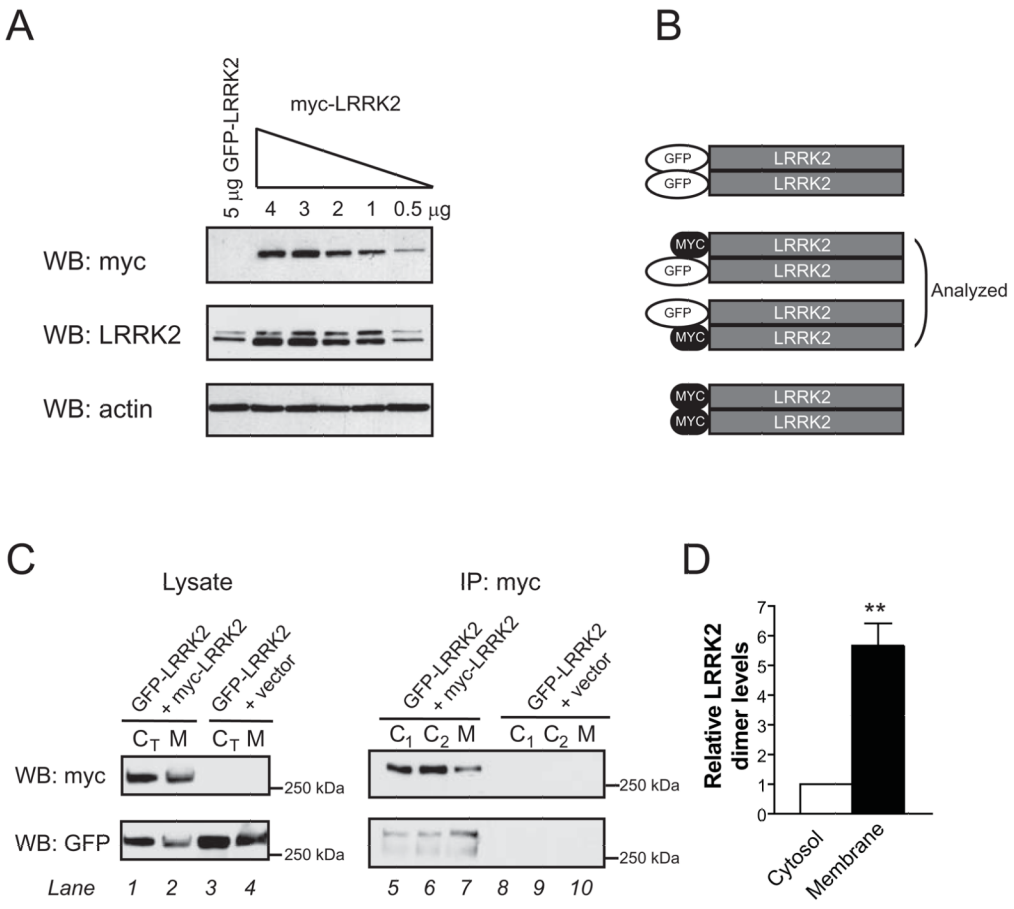

Figure 4. Heterologous co-immunoprecipitation confirms an enrichment of the LRRK2 dimer at the membrane

(**A**) To optimize the heterologous co-immunoprecipitation (co-IP) system, the amount of myc-LRRK2 DNA was titrated to match the expression levels of GFP-LRRK2. Transfection with 0.5 µg of myc-LRRK2 led to similar levels of LRRK2 protein as 5 µg of GFP-LRRK2.

(**B**) A schematic depicting possible LRRK2 dimers after transfection with GFP-LRRK2 and myc-LRRK2 plasmids. Co-IP of heterologously tagged constructs allows quantification of GFP-LRRK2/myc-LRRK2 heterodimer, which at equal levels of both proteins will likely represent 50% of total dimer.

(**C**) Cytosol and membrane fractions from cells co-expressing GFP-LRRK2 and myc-LRRK2 (*lanes 1–2)* or GFP-LRRK2 and an empty vector (*lanes 3–4)* were used for IP using a high affinity myc resin. GFP-LRRK2 is co-IPed only in the presence of myc-LRRK2 (*lanes 5–9)*, confirming specificity of IP. Higher levels of GFP-LRRK2 are pulled down from membrane extracts (*lane 7)*, despite lower levels of myc-LRRK2 in the same IP, suggesting an enrichment of LRRK2 dimer at the membrane. Identical results from two independent samples (C_1, C_2) using the same total cytosolic fraction (C_T) illustrate the low variability of this assay.

(**D**), Levels of LRRK2 heterodimers are 5.7-fold higher in membrane extracts (Mean ± SEM, $p = 0.01$, n = 3, unpaired t-test). The relative dimer levels were quantified by measuring the band intensity of co-IPed GFP-LRRK2 divided by the intensity of IPed myc-LRRK2. The value for cytosol was arbitrarily set as 1. ** $p \leq 0.01$.

NIH-PA Author Manuscript

NIH-PA Author Manuscript

NIH-PA Author Manuscript

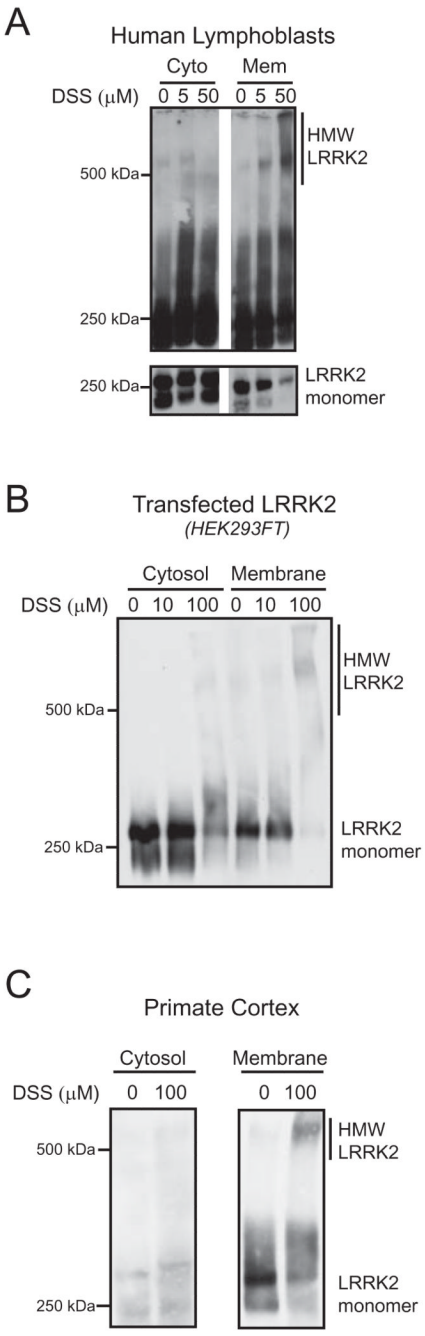

Figure 5. Membrane bound LRRK2 can be crosslinked more efficiently into HMW complexes than cytosolic LRRK2

Crosslinking with DSS of endogenous or transfected LRRK2 leads to formation of HMW complexes in membrane fractions (Mem), but not in cytosol (Cyto). Extracts from human lymphoblasts (**A**), HEK293FT cells transfected with LRRK2 (**B**), and non-human primate cortex (**C**) were analyzed.

NIH-PA Author Manuscript

NIH-PA Author Manuscript

NIH-PA Author Manuscript

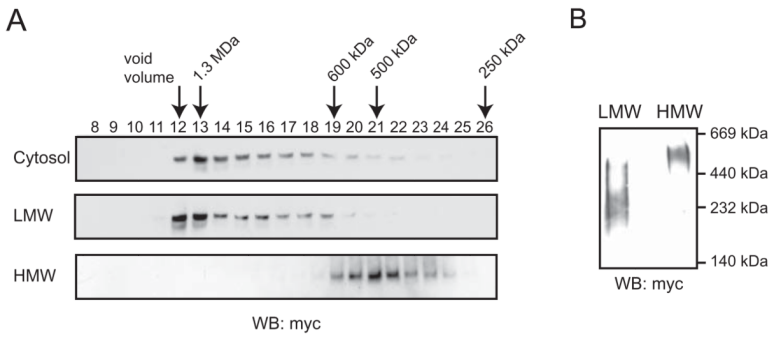

Figure 6. Analysis of LRRK2 by size exclusion chromatography and Blue-Native PAGE

(**A**) Cytosolic LRRK2 and LMW LRRK2 (both monomer) elute similarly from a Superdex 200 column, at ~ 1.3MDa, while HMW LRRK2 (LRRK2 dimer) elutes at ~ 500kDa. (**B**) LMW LRRK2 from the glycerol gradient separation subsequently migrates on BN-PAGE as a LRRK2 monomer, whereas migration of HMW LRRK2 corresponds to a dimer. Two commercially available molecular weight standards were used on the Blue-Native PAGE to estimate LRRK2 molecular weight (see Figure S4).

NIH-PA Author Manuscript

NIH-PA Author Manuscript

NIH-PA Author Manuscript

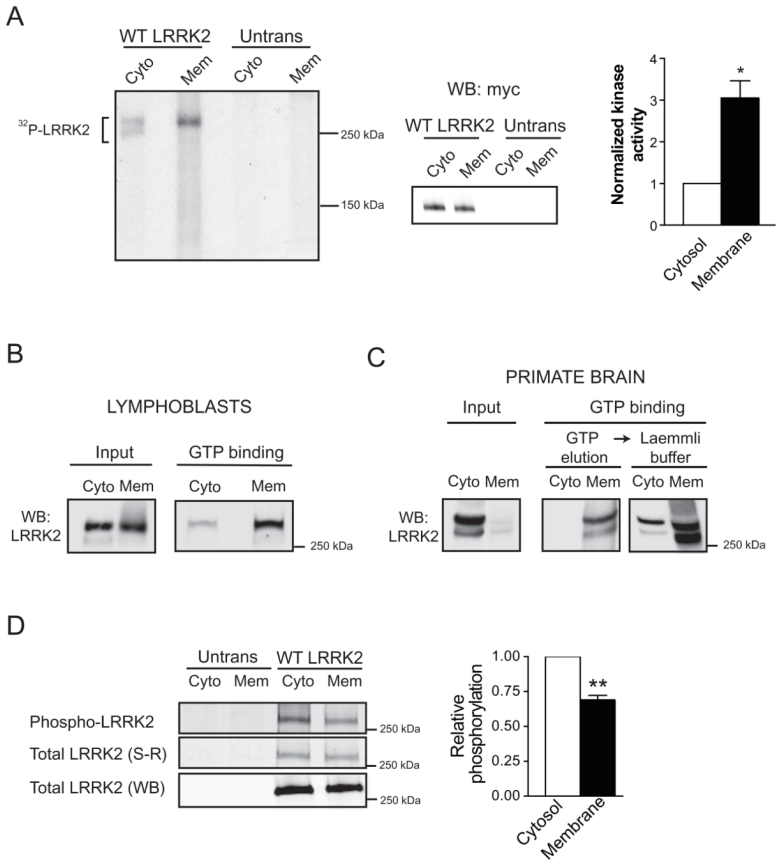

Figure 7. Membrane-associated LRRK2 is biochemically distinct from cytosolic LRRK2

(**A**) Membrane-associated LRRK2 exhibits greater *in vitro* kinase activity than cytosolic LRRK2. Cytosol and membrane fractions from HEK293FT cells transfected with wild-type myc-LRRK2 or from untransfected cells (Untrans) were used for myc IP and subsequent LRRK2 autophosphorylation assay. Membrane and cytosolic fractions were normalized to achieve similar levels of LRRK2 in the kinase reaction, shown by Western blot. Autoradiograph of an SDS-PAGE gel separating the LRRK2 autophosphorylation reaction products show increased incorporation of radioactive ^{32}P into LRRK2 from membrane extracts. LRRK2 from the cytosolic fraction migrates on this gel as a doublet; both bands correspond to full-length LRRK2 and were included in the analysis. Relative LRRK2 kinase activity is 3.1-fold greater from membrane fraction than from cytosol (Mean ± SEM, p = 0.04, n = 3, unpaired t-test). * $p < 0.05$.

(**B**) Membrane-associated LRRK2 from human lymphoblasts binds GTP more efficiently than cytosolic LRRK2. The levels of LRRK2 were normalized in the input and equal volumes of inputs were used for each analysis, with three independent experiments demonstrating similar results.

(**C**) Membrane-associated LRRK2 extracted from primate brain binds GTP more efficiently than cytosolic LRRK2. LRRK2 was first eluted with GTP from the resin and subsequently the GTP binding resin was boiled in Laemmli buffer. Samples used for the assay were protein and volume normalized, a representative experiment (n =3) is shown.

(**D**) Membrane-associated LRRK2 is phosphorylated to a lesser extent than cytosolic LRRK2. Cytosolic and membrane fractions from untransfected cells (Untrans) or cells transfected with wild-type myc-LRRK2 (WT LRRK2) were IPed with myc resin, and analyzed for phosphorylation using Pro-Q® Diamond Phosphoprotein gel stain (Phospho-

LRRK2). The relative levels of LRRK2 phosphorylation were quantified by normalizing the intensity of phospho-LRRK2 (phospho-protein stain) to the levels of total LRRK2 protein by SYPRO® Ruby stain (total LRRK2 S-R). Relative LRRK2 levels were further confirmed by analyzing a small aliquot of each fraction by Western blot (total LRRK2 WB). (Mean ± SEM, $p = 0.01$, n = 3, unpaired t-test). ** $p \leq 0.01$

NIH-PA Author Manuscript
NIH-PA Author Manuscript
NIH-PA Author Manuscript

NIH-PA Author Manuscript

NIH-PA Author Manuscript

NIH-PA Author Manuscript

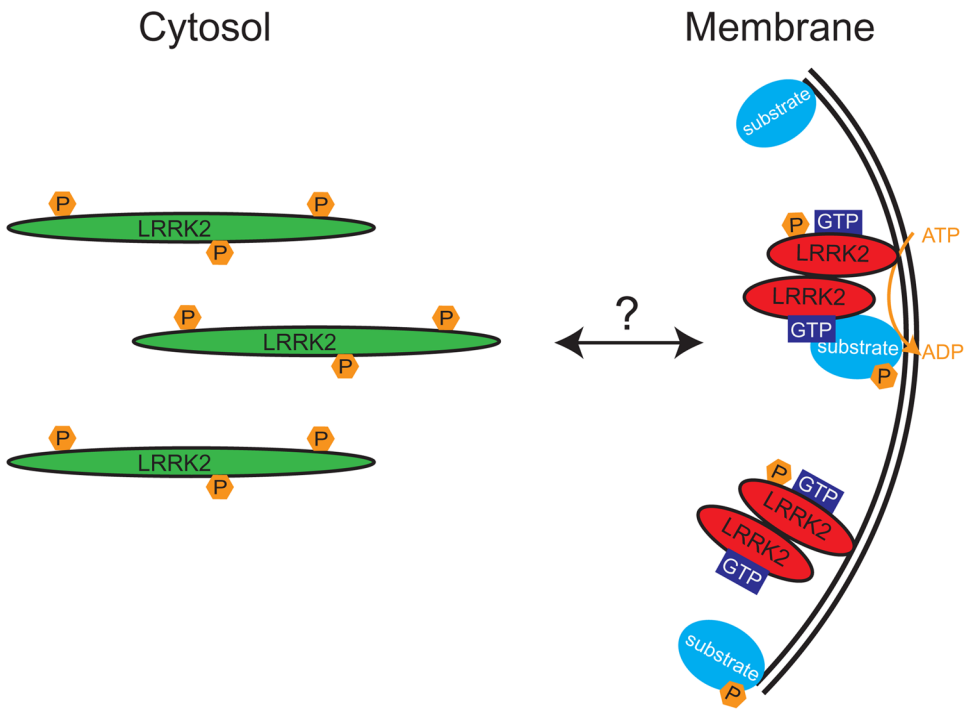

Figure 8. Schematic representation of proposed model of LRRK2 dimer assembly and kinase regulation

Using both endogenous and exogenous LRRK2, we have observed that membrane-associated LRRK2 is substantially enriched for LRRK2 dimer, whereas cytosolic LRRK2 is present mostly as a monomer. Membrane-associated LRRK2 possesses greater kinase activity, an increased propensity to bind GTP, and is relatively dephosphorylated, compared to cytosolic LRRK2. We propose a model, where LRRK2 exists mostly as a monomer in the cytosol that can translocate to membrane where it dimerizes, becomes more active and subsequently phosphorylates its substrates. The similarities of this model to the established regulation of other kinases (and GTPases) suggest that membrane translocation and dimerization may be reversible and tightly controlled.